Photothermal Release of Single-Stranded DNA from the Surface of Gold Nanoparticles Through Controlled Denaturing and Au—S Bond Breaking

Lester Poon,[‡] Wesley Zandberg,[†] Dennis Hsiao,[†] Zach Erno,[†] Dipankar Sen,[‡] Byron D. Gates,[†,*] and Neil R. Branda[†,*]

[†]4D LABS, Department of Chemistry and [‡]Department of Molecular Biology and Biochemistry, Simon Fraser University, 8888 University Drive, Burnaby, British Columbia, Canada, V5A 1S6

Gene and antisense therapy has the potential to revolutionize the treatment of cancer and other diseases by providing patients with functioning replacements for defective genes or with oligonucleotides that deactivate harmful gene products. The future use of this type of therapy in clinical settings hinges primarily on whether gene delivery vehicles (vectors) can be designed with the following capabilities: (1) They must be able to selectively transport oligonucleic acid-based therapeutics to diseased tissues; (2) they must protect the oligonucleotides from physiological degradation while en route; and 3) there should be a mechanism to facilitate the 'on-command' release of the gene payload when the target site is reached. The vast majority of gene therapy research reported over the past two decades has focused on viral vectors whose evolved natural machinery carries out the targeted delivery and release of therapeutic genes.[1] However, several practical issues concerning viral vectors, such as the difficulty in manufacturing them and their association with serious health risks (insertional mutagenesis[2] and lethal hypersensitivity[3]), justify the growing interest in synthetic, nonviral delivery vectors (liposomes and nanoparticles) as alternatives.[4-6]

Gold nanoparticles are particularly appealing candidates as vehicles for gene delivery because they exhibit low cytotoxicities when tuned to suitable sizes and coated with appropriate ligands.[7-9] (An inappropriate choice of size and ligand can lead to nanoparticles exhibiting cytotoxic effects.)[10,11] Gold nanoparticles are readily internalized by cells[12-14] and can be easily derivatized with multiple molecular species to simultaneously provide biological compatibility, enhanced cell-targeting,[15,16] and immunoevasive properties.[17,18] Additionally, gold nanoparticles possess intense optical absorbance bands (corresponding to excitation of localized surface plasmons) that can be tuned throughout the visible and near-infrared regions of the electromagnetic spectrum based on the size, shape, and composition of the particle.[19,20] How these bands impact the use of nanoparticles in the controlled delivery of therapeutics lies in the fact that when light of appropriate wavelengths is absorbed, it is converted into heat, which can be localized close to the nanoparticle's surface (the photothermal effect).[16,21] Originally, this phenomenon was used in biologically relevant studies to

ABSTRACT Photothermal release of DNA from gold nanoparticles either by thermolysis of the Au—S bonds used to anchor the oligonucleotides to the nanoparticle or by thermal denaturation has great therapeutic potential, however, both processes have limitations (a decreased particle stability for the former process and a prohibitively slow rate of release for the latter). Here we show that these two mechanisms are not mutually exclusive and can be controlled by adjusting laser power and ionic strength. We show this using two different double-stranded (ds)DNA—nanoparticle conjugates, in which either the anchored sense strand or the complementary antisense strand was labeled with a fluorescent marker. The amounts of release due to the two mechanisms were evaluated using fluorescence spectroscopy and capillary electrophoresis, which showed that irradiation of the decorated particles in 200 mM NaOAc containing 10 mM Mg(OAc)$_2$ with a pulsed 532 nm laser operating at 100 mW favors denaturation over Au—S cleavage to an extent of more than six-to-one. Due to the use of a pulsed laser, the process occurs on the order of minutes rather than hours, which is typical for continuous wave lasers. These findings encourage continued research toward developing photothermal gene therapeutics.

KEYWORDS: nanostructures · photothermal · oligonucleotides · drug delivery · controlled release

cause cell death.[22] It has more recently been harnessed as a means to optically elicit the release of small molecules anchored to the nanoparticle surface in a manner that offers excellent spatial and temporal control.[23] The fact that the light used as the photothermal trigger can be tuned to lie in low-energy regions of the visible or near-infrared spectrum offers the added benefits of deeper tissue penetration and fewer detrimental accompanying effects than can be achieved with high-energy visible or UV light.

Reports of the photothermal effect being used to facilitate the controlled release of therapeutic oligonucleotides from gold nanostructures have only recently begun to appear.[24−28] The first among these described the use of pulsed laser irradiation to elicit cleavage of the Au−S bond anchoring thiolated single-stranded (ss)DNA to the particle's surface.[25,26] This release mechanism is potentially problematic as it results in a decrease in the stability of the nanoparticles since the release process relies on the dissociation of the stabilizing surface ligands. (This instability will become apparent later in this paper.) Breaking the Au−S bond also releases free thiols, which may have detrimental effects in live cells. More recent photorelease strategies have sought to address these limitations by utilizing double-stranded (ds) DNA−nanoparticle conjugates in which only one of the two oligonucleotide strands is anchored to the nanoparticle surface through a Au−S bond.[27,28] Irradiation of these systems with continuous-wave (CW) lasers triggered the photothermal effect and raised the local temperature above the melting temperature (T_m) of the DNA duplex, which allowed the nonthiolated strand to dissociate into the surrounding medium while its complement remained attached to the nanoparticle. The appeal of this process is primarily that the nanoparticle remains unchanged after the photothermal and release events. This approach, however, is not without its own shortcomings. It generates relatively low photorelease efficiencies and requires irradiation periods that are nearly twice as long as the examples using pulsed lasers in order to attain measurable degrees of oligonucleotide release. Both limitations are presumably attributable to the characteristically lower power densities attainable by irradiation with CW *versus* pulsed lasers. There are two reported examples where pulsed laser irradiation was used to elicit rapid melting and reannealing of thiol-bound dsDNA in gold nanoparticle networks, which were supported based on the reversible shifts of the nanoparticles' absorbances.[29,30] The fact that reannealing was observed in these studies suggests some of the Au−S bonds anchoring the ssDNA to the nanoparticles remain intact after irradiation. However, neither study evaluated whether repeated photothermal denaturation would lead to system fatigue indicative of competitive Au−S bond cleavage.

A method that takes advantage of the efficient photothermal heating possible using pulsed lasers, but avoids the negative consequences of breaking the Au−S bonds anchoring a double-stranded oligonucleotide to the nanoparticle would be highly beneficial and is the focus of the experiments described in this paper.

In order to improve the relatively inefficient photorelease of ssDNA from dsDNA−gold nanoparticle conjugates, we undertook a series of studies where the conjugates' response to pulsed irradiation under varying conditions was examined. The effects of laser power and salt content on the amount of ssDNA released through a denaturation process instead of Au−S bond cleavage were the primary focus of our studies. We chose to quantify and compare the extent of release attributable to each mechanism by preparing the two different dsDNA−nanoparticle conjugates shown in Scheme 1 (a third conjugate will be discussed at the end of this paper). The first conjugate (**1**) is comprised of a fluorescently labeled antisense oligonucleotide hybridized to a complementary, thiolated sense strand anchored to the nanoparticle surface by an Au−S bond. In the other conjugate (**2**), the single-stranded DNA attached to the nanoparticle contains the luminescent tag, and its antisense complement is unlabeled. In both conjugates, emission from the luminescent tag should be quenched due to its close proximity to the metal nanoparticle and the existence of a nonradiative relaxation of the dye's excited state through energy and/or electron transfer. The appearance of fluorescence after stimulation is, therefore, a convenient probe for successful release as we have demonstrated in a previous publication.[23] Using this photothermally induced emission, the two conjugates will help identify whether denaturing of the double helix or Au−S bond breaking is the dominant mechanism.

Scheme 1 shows all possible photothermal release mechanisms and how they can be distinguished from one another. When an increase in fluorescence intensity is observed after conjugate **1** is irradiated with the appropriate light to induce the photothermal effect, either of the two mechanisms has occurred. Assuming the heat generated at the surface of the nanoparticle is higher than the melting temperature of the dsDNA, denaturation of the duplex released the fluorescently labeled antisense oligonucleotide from the nanoparticle and into solution (path A). An alternative (path C) is that irradiation resulted in cleavage of the Au−S bond anchoring the thiolated sense oligonucleotide onto the nanoparticle. The outcome of this process is the release of the entire dsDNA or a mixture of single-stranded oligonucleotides.

The situation is different for conjugate **2**. Because fluorescence arises only from the tag attached to the thiolated sense strand, which is also anchored to the nanoparticle surface, any fluorescence observed after
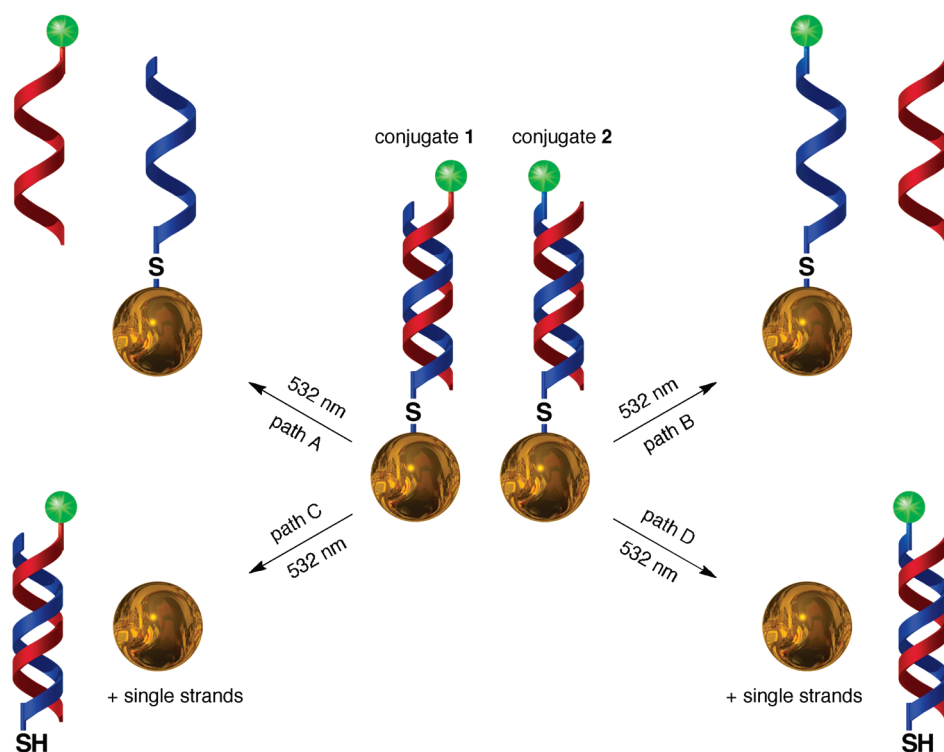
Scheme 1. Photothermal release of fluorescently labeled DNA from dsDNA−nanoparticle conjugates (1 and 2) attached to the surfaces of gold nanoparticles.[a] [a]Exposure to pulsed laser irradiation with 532 nm light elicits release of genetic material by denaturation (paths A and B) or by Au−S bond cleavage (paths C and D), which can be distinguished from one another by selectively labeling one strand within the dsDNA with a luminescent marker.

the release event can only be due to the breaking of the Au−S bond (path D). If there is no observable emission and the heat generated from the photothermal process is enough to denature the dsDNA (as indicated from the results using conjugate 1), then the conditions are optimized to induce release of the antisense oligonucleotide while retaining the sense oligonucleotide on the nanoparticle (path B). By comparing the results from the experiments using conjugates 1 and 2, the relative efficiencies of two general photorelease reactions can be assessed under a variety of conditions, and those that enhance only the release of the antisense oligonucleotide can be optimized.

In this paper, we report our efforts to develop a method to elicit efficient photothermal release of a 14-residue antisense oligonucleotide from a thiolated 17-residue sense strand anchored to the surfaces of 16 nm gold nanoparticles in a manner that minimizes Au−S bond cleavage and maximizes denaturation of the dsDNA. The extent to which each process occurs during the release event was probed using fluorescence spectroscopy and capillary electrophoresis of fluorescently labeled oligonucleotides according to the outline in Scheme 1. Here we highlight that the extent to which each of the two photothermal release mechanisms occurs is highly dependent on the power of the laser used to stimulate the nanoparticles and the nature of the cationic salt present in solution. When both are taken into consideration, the primary release event is denatur-

ation of the dsDNA and selective release primarily of the antisense oligonucleotide.

RESULTS AND DISCUSSION

The citrate-coated 16 nm gold nanoparticles used in our studies were synthesized using reported methods.[31,32] These nanoparticles were characterized with optical spectroscopy and electron microscopy, which gave results corresponding to the proposed size and composition and a relatively good monodispersity (Figure 1). We constructed dsDNA−nanoparticle conjugates 1 and 2 by following previously published protocols as outlined in Scheme 2.[33] The general multistep route involves first attaching the corresponding 17-mer 5′-thiolated sense strands to the surfaces of the citrate-coated 16 nm gold nanoparticles through a ligand-exchange process, followed by hybridization of the ssDNA−nanoparticle conjugates to their complementary antisense strands. Using this route, either the unlabeled t-17SS (HS−C_6−5′TTTCATAGTTGACCTCT3′) or t-17SS-FAM having the same sequence and a luminescent carboxyfluorescein tag attached to its 3′ end (HS−C_6−5′TTTCATAGTTGACCTCT3′−6-FAM) was used to decorate the gold nanoparticles by first incubating their respective, protected disulfides with tris(2-carboxyethyl)phosphine in phosphate buffer to release the free thiol, followed by desalting (MicroSpin column) to remove the reducing agent. The ssDNA−nanoparticle conjugates were prepared by treating
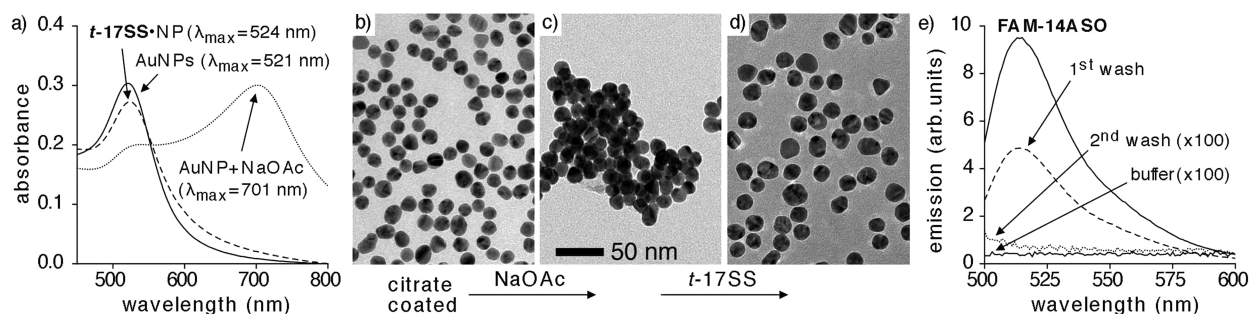
Figure 1. (a) Changes in the UV−vis absorption spectrum when an aqueous dispersion of 16 nm gold nanoparticles (solid line) is treated with NaOAc (dotted line) and then with the unlabeled thiolated oligonucleotide (t-17SS) (dashed line), showing a large red shift of the SPR band indicative of aggregation for the former and a small red shift indicative of ligand exchange for the latter. The TEM images of (b) untreated 16 nm citrate-coated gold nanoparticles, and the same nanoparticles treated with (c) 100 mM NaOAc and (d) thiolated ss-DNA (t-17SS) show aggregation and redispersion of the nanoparticles, respectively. (e) Emission spectra (λ_{ex} = 490 nm) for an aqueous buffered solution of the labeled antisense oligonucleotide (FAM-14ASO) (solid line), the supernatant obtained when the same solution is incubated for 24 h with ssDNA−nanoparticle complexes followed by washing and centrifugation (dashed and dotted lines), and the buffer used for washing (baseline).

aqueous dispersions of 16 nm gold nanoparticles with excess amounts (more than 100 mol equiv) of freshly activated t-17SS or t-17SS-FAM in phosphate buffer, then aqueous NaOAc in order to increase DNA loading onto the nanoparticle.[34] In both cases, unbound ssDNA was removed by a repetitive (three times) centrifugation−resuspension process using either a phosphate buffer containing NaOAc (100−200 mM) or a mixture of NaOAc (200 mM) and MgOAc (10 mM). The choice of buffer and added salt will become clear when

the photorelease experiments are discussed later in this paper.

The citrate-ssDNA ligand exchange process was monitored using UV−vis absorbance spectroscopy. This is feasible due to the fact that replacing the citrate capping ligand with the thiolated sense oligonucleotide resulted in a small but observable red shift of the nanoparticle's surface plasmon resonance (SPR) band (Figure 1a).[25] Transmission electron microscope imaging shows that the 16 nm citrate-coated nanoparticles
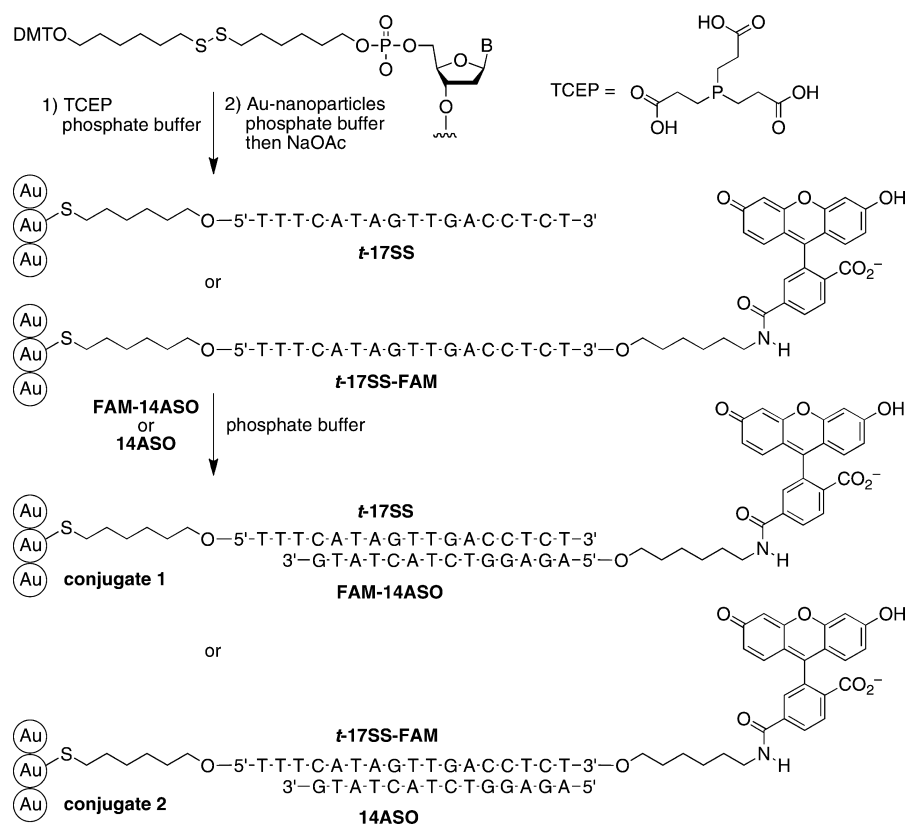
Scheme 2. Synthesis of fluorescently labeled dsDNA−nanoparticle conjugates (1 and 2) used in all our studies.[a] [a]The synthesis involves: (1) release of the 'free' thiol of modified sense ssDNA (t-17SS or t-17SS-FAM), (2) ligand exchange of the ssDNA and citrate on the surface of 16 nm gold nanoparticles, and (3) hybridization of the decorated ssDNA−nanoparticle complexes to their complementary antisense strands (FAM-14ASO and 14ASO).

are stable and well-dispersed (Figure 1b and Supporting Information). However, the high concentrations of salt (NaOAc) required to enhance the loading of the oligonucleotides onto the nanoparticle had a detrimental effect on the nanoparticle stability, as illustrated by the significant aggregation shown in Figure 1c. This is further supported by the 180 nm bathochromic shift in the nanoparticles' absorbance peak following treatment with NaOAc, which is a documented consequence of aggregation.[35] As previously mentioned in this paper, ligand exchange in buffered systems introduces a major limitation of nanoparticles in medical applications, where aggregation is undesirable. The replacement of citrate ligands by acetates clearly demonstrates this claim and supports the justification for minimizing Au−S bond breaking in the photothermal release process as it will have a similar effect. Figure 1d shows that when the nanoparticles are decorated with ssDNA (t-17SS), they regain their stability and are well dispersed even in the highly concentrated salt solutions, which is not possible without the shielding effect of conjugated DNA. Similar dispersion was observed for the labeled ssDNA (t-17SS-FAM) as well as the two dsDNA systems (conjugates **1** and **2**), as shown in the Supporting Information.

The final dsDNA−nanoparticle conjugates (**1** and **2**) were prepared by hybridizing the ssDNA−nanoparticle complexes to their complementary antisense oligonucleotides, the luminescent 5′ carboxyfluorescein-labeled FAM-14ASO (6-FAM-5′AGAGGTCTACTATG3′) in the case of conjugate **1** and the unlabeled 14ASO (5′AGAGGTCTACTATG3′) for conjugate **2**. Hybridization was achieved by heating the aqueous dispersions at 80 °C for 3 min, followed by cooling them to room temperature over the span of 1 h in order to overcome nonspecific base pairing prior to duplex formation. The excess of the complementary strand was removed by successive centrifugation and resuspension processes as described for the original ssDNA−nanoparticle complexes. The hybridization process was monitored by fluorescence spectroscopy in the case of FAM-14ASO (Figure 1e) where the emission from a buffered solution containing only labeled antisense ssDNA is significantly reduced when treated with the ssDNA−nanoparticle complex and incubated for 24 h. The spectra in Figure 1b clearly illustrate uptake of FAM-14ASO by the ssDNA−nanoparticle complex. The decrease in fluorescence upon duplex formation at the nanoparticle surface is consistent with distance-dependent luminescence quenching by the gold.[23] A third conjugate containing both labeled DNA strands (t-17SS-FAM and FAM-14ASO) was also prepared following the same protocol. It similarly showed little observable fluorescence even with two fluorescent components per DNA duplex. This doubly labeled conjugate will be discussed later in this paper when the re-
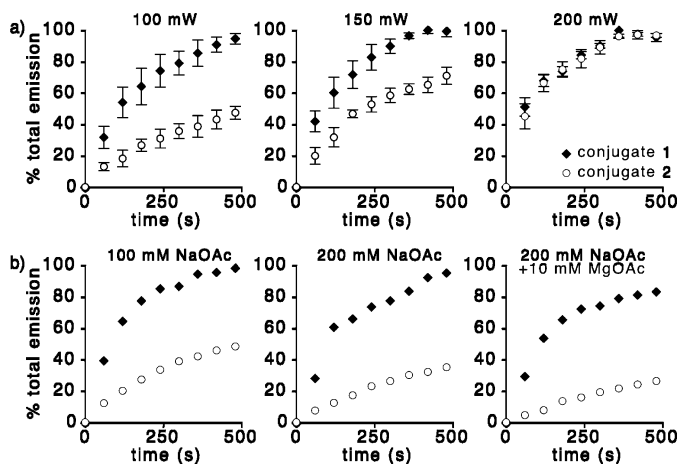

Figure 2. Changes in the fluorescence intensity (λ_{em} = 513, λ_{ex} = 490 nm) of aqueous dispersions of dsDNA−nanoparticle conjugates **1** (◆) and **2** (○) after irradiation with a 532 nm pulsed laser (10 Hz, 4 ns) as the laser power (a) and salt content (b) are varied. In (a) the salt concentrations are held constant at 100 mM NaOAc. Emission intensities are reported as percentages of the total emission measured on identical samples after they were treated with 0.5 M dithiothreitol to induce quantitative Au−S bond cleavage and detachment of the labeled sense strand from the nanoparticle.

sults from the capillary electrophoresis experiments are presented.

Figure 2 shows the results from the photothermal release experiments, where fluorescence quenching of the FAM label by the SPR band of the nanoparticle is reduced, and the emission is turned 'on' as soon as the dye is released from the nanoparticle's surface, thus providing a means to monitor the success of the photothermal release by comparing the fluorescence before and after stimulation. For all graphs in Figure 2, the black diamonds correspond to changes in luminescence as a result of irradiating conjugate **1**, while the open circles correspond to changes arising from irradiating conjugate **2**. Because the goal of these studies is to use a pulsed laser as the irradiation source to elicit rapid photothermal release without compromising the integrity of the gold nanoparticles or the Au−S bond, the first set of experiments focused on varying the laser power (Figure 2a). In all experiments, the fluorescence is normalized as a percent relative to the maximum fluorescence attainable assuming all fluorescently labeled ssDNA (t-17SS-FAM and FAM-14ASO) is released from the surface. This value was obtained by chemically removing all DNA using dithiothreitol and measuring the total emission in identical solutions to those used for each photorelease experiment.[34]

As is clearly demonstrated by the data in Figure 2a, the percent of DNA released from dsDNA−nanoparticle conjugate **1** is significantly greater than that for conjugate **2** as long as the laser intensities are kept below 200 mW. At this power, both conjugates appear to release labeled DNA to the same extent. Irradiating either conjugate with a laser at powers below 100 mW resulted in little to no observable changes in fluorescence (not shown). At all powers where photothermal release oc-
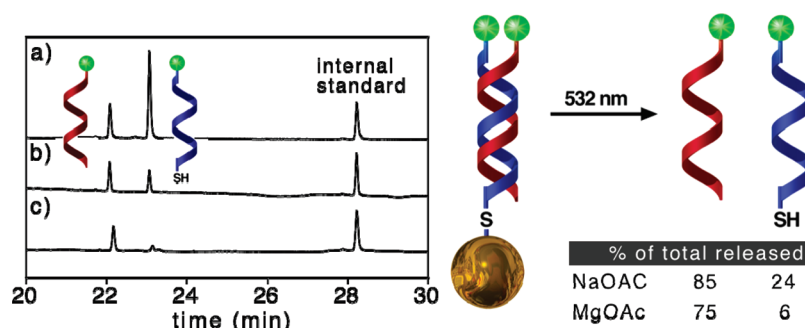
Figure 3. Quantitative analysis and identification of photorelease products *via* denaturing capillary electrophoresis. Chromatogram depicting elution of *t*-17SS-FAM and FAM-14ASO following treatment of the dsDNA−nanoparticle conjugates with (a) dithiothreitol, (b) pulsed laser irradiation at 100 mW in the presence of 100 mM NaOAc, and (c) irradiation in the presence of 200 mM NaOAC containing 10 mM Mg(OAc)$_2$. Each release product is quantified as a percentage of the total amount generated in solution established in trace (a).

curs (100−200 mW), the amount of fluorescence generated after conjugate **1** is irradiated for at least 8 min is equal to the total amount of label decorated onto the nanoparticle (100% emission compared to the that of equivalent solutions treated with dithiothreitol). What changes with laser power is the amount of fluorescence obtained when conjugate **2** is irradiated. Decreasing the laser power (from 150 to 100 mW, for example) significantly reduces the amount of released, labeled DNA (t-17SS-FAM), as attested by the greatly reduced emission after the same period of time. Since the emission in the case of conjugate **2** can arise only from breaking the Au−S bond and releasing the thiolated strand, while emission from conjugate **1** can arise from either mechanism, it can be assumed that the contribution of Au−S bond breaking to the entire release process becomes much less with lower laser powers. These experiments strongly suggest that irradiation powers close to 100 mW trigger the nanoparticles to generate photothermal heat that is greater than the T_m of the dsDNA duplex (greater than 60−70 °C)[36] while minimizing the contribution of Au−S bond breaking. The similarity in the amount of labeled DNA that is released from conjugate **1** when any of three laser powers is used suggests that any additional emission resulting from the release of the fully assembled dsDNA has little effect. Therefore, it is likely photothermal denaturation occurs prior to Au−S bond breakage even for conjugate **1**, in which release by either mechanism is feasible.

In the context of optimizing denaturation over Au−S bond breaking in the photothermal process, we were also motivated by reports of 'salt shielding' being used to increase DNA loading onto nanoparticles by decreasing the electrostatic repulsion between the oligonucleotide strands.[27,33,34] Our logic is as follows: Photothermal release by breaking the Au−S bond (in either conjugate) may be thermodynamically favorable in order to reduce the electrostatic repulsion between adjacent dsDNA duplexes on the nanoparticle surface. Reducing this repulsion by adding appropriate cations may also stabilize the decorated nanoparticles, reducing the strain on each Au−S bond and raising the acti-

vation energy required for Au−S bond cleavage. This suggestion is supported by the results of the photothermal release experiments shown in Figure 2b.

While all experiments in Figure 2a were performed on solutions of the dsDNA−nanoparticle conjugates containing the same amount of salt (100 mM NaOAc), those shown in Figure 2b contain varying concentrations and nature of the additive, while the laser power is kept constant (100 mW). Doubling the concentration of NaOAc (to 200 mM) resulted in only a modest decrease in the overall photorelease efficiency, however, the contribution from breaking the Au−S bond was reduced to a greater extent. Both observations are consistent with reported protocols that utilize 'salt shielding' as a means to simultaneously elevate the T_m values of DNA duplexes and to increase the stability of the Au−S bonds.[27,34] These effects were increased when 10 mM Mg(OAc)$_2$ was added to the solutions already containing 200 mM NaOAc. The further drop in the extent of Au−S bond breaking is consistent with the heightened degree of electrostatic shielding afforded by the divalent Mg^{2+} ion.

Finally, in order to quantitatively assess the relative amount of DNA released due to photothermal cleavage of the Au−S bond, we prepared a third DNA−nanoparticle conjugate incorporating FAM-14ASO hybridized to t-17SS-FAM. One sample was treated with dithiothreitol in order to elicit complete dissociation of all DNA strands from the nanoparticle surface (Figure 3a), another was exposed to pulsed laser irradiation at 100 mW in the presence of 100 mM NaOAc (Figure 3b), and the third was irradiated at 100 mW in 200 mM NaOAc containing 10 mM Mg(OAc)$_2$ (Figure 3c). All three samples were examined by analytical fluorescent capillary electrophoresis under denaturing conditions. Comparison of the three chromatograms with an internal standard and with the purchased DNA oligomers confirms that under each set of release conditions the DNA oligomers remain chemically unchanged. Moreover, these data indicate a four-fold decrease in the amount of Au−S cleavage when photorelease is performed in the presence of the

divalent Mg^{2+} salt, which is consistent with our previous data.

CONCLUSIONS

We have developed a method to efficiently elicit the release of single-stranded (ss)DNA from gold nanoparticles by photothermal dehybridization of a thiolated duplex in response to pulsed laser irradiation. Using fluorimetry we have quantified the extent of photorelease that occurs via Au−S bond cleavage, and we have shown that it can be minimized by using laser powers no greater than 100 mW and by shielding the electrostatic repulsion among strands. Furthermore, we have confirmed using capillary electrophoresis that neither the antisense nor the sense strands are chemically modified during photorelease.

METHODS

General. All oligonucleotides were purchased from the University of Calgary DNA Services (www.ucalgary.ca/dnalab) in 200 nmol quantities as DMTO-modified disulfides (see Scheme 2) and received as dry solids. The melting temperatures (T_m) for the ds-DNA complexes are reported by the supplier as 59 °C in aqueous 100 mM NaOAc, 63 °C in aqueous 200 mM NaOAc, and 67 °C in aqueous 200 mM NaOAc/10 mM $MgSO_4$. Supplies for capillary electrophoresis were purchased from Beckman-Coulter. Water used in oligonucleotide manipulations and in the synthesis and purification of the nanoparticles was obtained from a Barnstead NANOpure Diamond water purification system (18 MΩ). All other chemicals were purchased from Sigma Aldrich and used without purification. Centrifugation was carried out using an Eppendorf Microcentrifuge 5415D, and spin column chromatography was performed using MicroSpin G-50 columns (G. E. Healthcare). UV−vis absorbance and fluorescence spectra were acquired using a Varian Cary 300-Bio spectrophotometer and a Photon Technology International QuantaMaster spectrometer, respectively. Capillary electrophoresis was performed using Beckman-Coulter ProteomeLab PA800 with a 488 nm Ar laser-induced fluorescence detector. Transmission electron microscopy (TEM) images were taken on an FEI Tecnai G2 STEM. Photorelease experiments were carried out using a nanosecond Nd:YAG (neodymium-doped yttrium aluminum garnet, $Nd:Y_3Al_5O_{12}$) PL8000 laser (Continuum).

Synthesis of Gold Nanoparticles. Using a modified version of the Turkevich method,[32] $HAuCl_4$ (25 mg, 7.5 μmol) was dissolved in water (50 mL) with magnetic stirring, then heated to reflux, and subsequently treated with aqueous trisodium citrate (4.5 mM, 10 mL). Heating was continued for 15−20 min until the color of the solution had changed from yellow to red, at which time, the reaction mixture was allowed to slowly cool to room temperature without stirring. The resulting solution of gold nanoparticles was used without further purification for later experiments. Based on the TEM analysis, the average particle size was 16 ± 2 nm (Figure 1b). UV−vis absorbance spectroscopy indicates a nanoparticle concentration of 1.25 nM ($\varepsilon = 2.4 \times 10^8$ L $mol^{-1}cm^{-1}$ at $\lambda_{max} = 521$ nm, Figure 1a).[34]

Activation of Thiolated ssDNA. A solution containing DMTO-t-17SS (DMTO$−C_6−S−S−C_6−$5′TTTCATAGTTGACCTCT3′) or DMTO-t-17SS-FAM (DMTO$−C_6−S−S−C_6−$5′TTTCATAGTTGACCTCT3′$−$6-FAM) (200 nmol) was prepared in Tris−EDTA buffer (2.00 mL, 10 mM Tris, 1 mM EDTA, pH 7.4). A 20 μL aliquot of this solution was treated with phosphate buffer (3 μL, 1.0 M, pH 7.5), aqueous tris-(2-carboxyethyl)phosphine (3 μL, 300 mM), and water (4 μL). The reaction mixture was allowed to stand at room temperature for 1 h, at which time it was desalted by spin-column chromatography (MicroSpin G-50 columns, G. E. Healthcare) to remove the reducing agent to yield 40 μL of the oligonucleotide solution. The resulting solution was treated with fresh phosphate buffer (1 μL) and analyzed by UV−vis absorbance spectroscopy. The oligonucleotide concentration was determined to be 18 μM based on extinction coefficients provided by the vendor (154 600 L mol^{-1} cm^{-1} at $\lambda_{max} = 260$ nm for both t-17SS and t-17SS-FAM).

Synthesis of ssDNA−Nanoparticle Complexes. The attachment of DNA to the 16 nm gold nanoparticles was accomplished following a previously published protocol.[31] The previously prepared solution of the 16 nm gold nanoparticles (3.00 mL, 1.25 nM) was treated with the appropriate amount of the activated thiolated ssDNA (41 μL, 18 μM). The resulting mixture was allowed to stand at room temperature for 1 h, at which time phosphate buffer (1.0 M, pH 7.5) was added in six increments of 5 μL each over 1 h. The resulting mixture was allowed to stand at room temperature for 18 h when it was treated with phosphate buffer (10 mM) containing NaOAc (2.0 M) in 15 μL portions every 20 min, followed by sonication for 10 s, until a final NaOAc concentration of either 100 or 200 mM was reached, depending on the desired experimental conditions for subsequent photorelease (see below). If the sample was intended for photorelease in 10 mM $Mg(OAc)_2$, the solution was then treated with phosphate buffer solution (10 mM) containing $Mg(OAc)_2$ (1.0 M) in three 10 μL portions 20 min apart. Each addition was followed by sonication for 10 s. Samples that did not contain $Mg(OAc)_2$ were allowed to stand at room temperature for 22 h. All samples were purified by three cycles of centrifugation (30 min, 9.3k RCF, 4 °C) and resuspension in fresh phosphate buffer solution (1 mL) containing 100 mM, 200 mM, or 200 mM NaOAc and 10 mM $Mg(OAc)_2$, depending on the final salt concentration in the particular sample prior to centrifugation. Solutions that had been treated with t-17SS were analyzed by UV−vis absorbance spectroscopy. An absorbance maximum of 524 nm was observed (see Figure 1a) 3 nm longer than the absorbance maximum measured from the gold nanoparticles prior to treatment with the oligonucleotide, a feature characteristic of bond formation between thiols and gold nanoparticles.

Synthesis of dsDNA−Nanoparticle Complexes. The appropriate antisense oligonucleotide (14ASO (5′AGAGGTCTACTATG3′) or FAM-14ASO (6-FAM−5′AGAGGTCTACTATG3′)) (200 nmol) was dissolved in Tris−EDTA buffer (2.00 mL, 10 mM Tris, 1 mM EDTA, pH 7.4). An aliquot of this solution (11 μL) was added to a 1 mL sample of the solution containing gold nanoparticles decorated with either t-17SS or t-17SS-FAM in the presence of 100 mM, 200 mM, or 200 mM NaOAc and 10 mM $Mg(OAc)_2$. The resulting mixture was sonicated for 10 s, then heated to 80 °C for 3 min, and allowed to cool to room temperature over 1 h upon standing. The solution was purified by three cycles of centrifugation (30 min, 9.3k RCF, 4 °C) and resuspension in fresh phosphate buffer solution (1 mL) containing 100 mM, 200 mM, or 200 mM NaOAC and 10 mM $Mg(OAc)_2$ depending on the salt concentration in the particular sample prior to centrifugation. The hybridization of FAM-14ASO to the nanoparticles decorated with t-17SS was monitored by solution fluorescence spectroscopy. Spectra were acquired from the supernatant that was collected following centrifugation, which showed a significant decrease in fluorescence intensity in comparison with measurements taken from an equimolar solution of FAM-14ASO to which none of the decorated nanoparticles had been added (Figure 1e). Fluorescence measurements from the supernatant collected following the second and third centrifugation cycles show further decreases in emission, confirming the stability of the nanoparticle-bound duplex in solution prior to irradiation.

Photorelease Experiments. In quartz cuvettes, solutions of dsDNA−nanoparticle conjugate **1** or **2** in 1.0 mM phosphate buffer containing 100 mM, 200 mM, or 200 mM NaOAc plus 10 mM $MgOAc_2$, depending on the experiment, were exposed to pulsed laser radiation (532 nm, 10 Hz, 100 mW, 4 ns) for 60 s intervals with a beam 5 mm wide. The solutions containing 100 mM NaOAc were also irradiated using 150 and 200 mW laser powers with 5 mm beam widths. After each interval, an emission spectrum from 500−600 nm was acquired from the irradi-

ated sample (λ_{ex} = 490 nm). Irradiation was then repeated until no significant change in fluorescence intensity was observed. The fluorescence measurements from each sample were later analyzed as percentages of a maximum fluorescence corresponding to photothermal release of all fluorescent ligands attached to the nanoparticles, which was determined by treating an aliquot from each sample with 0.5 M dithiothreitol.

The solutions of dsDNA−nanoparticle conjugates bearing a fluorescent marker on each strand that were intended for subsequent capillary electrophoretic analyses were treated differently. Prior to irradiation, 3 mL of the sample prepared as described above in phosphate buffer containing either 100 or 200 mM NaOAc and 10 mM MgOAc$_2$ was centrifuged (16.1k rcf for 30 min at 4 °C), and the resulting pellet was resuspended in 20 μL of the conjugate solution. These solutions were transferred to quartz microcuvettes and irradiated as described above in three 60 s intervals at a laser power of 100 mW, then centrifuged (9.3k rcf). The supernatant was removed and desalted using MicroSpin G-50 columns (G. E. Healthcare), then stored at −20 °C prior to analytical capillary electrophoresis.

Analytical Capillary Electrophoresis (CE). Fluorescein labeled ssDNA oligomers were resolved by CE. All buffer and acrylamide gel components and coated DNA capillaries were prepared from a ssDNA 100-R kit and utilized according to the manufacture's instructions. All samples were stored at −20 °C and thawed immediately prior to analysis by CE. Sample injection was carried out electrokinetically from the cathode with a potential of −4 kV applied for 4 s. Fluorescence data from irradiated samples were compared to fluorescence of samples cleaved by dithiothreitol to obtain percent values. Data analysis and peak integration/quantification were performed using 32 Karat 5.0 software (Beckman-Coulter).

Supporting Information Available: Additional electron microscopy images of the nanoparticles used in these studies. This material is available free of charge *via* the Internet at http://pubs.acs.org.

Note Added after ASAP Publication: This article posted ASAP on October 19, 2010. Figure 1 has been revised. There are also some minor corrections to the text. The correct version posted on October 28, 2010.

REFERENCES AND NOTES

1. Cao, S.; Cripps, A.; Wei, M. Q. New Strategies for Cancer Gene Therapy: Progress and Opportunities. *Clin. Exp. Pharmacol. Physiol.* **2010**, *37*, 108–114.
2. Uren, A. G.; Kool, J.; Berns, A.; van Lohuizen, M. Retroviral Insertional Mutagenesis: Past, Present and Future. *Oncogene* **2005**, *24*, 7656–7672.
3. Lehrman, S. Virus Treatment Questioned After Gene Therapy Death. *Nature* **1999**, *401*, 517–518.
4. Kaneda, Y.; Tabata, Y. Non-Viral Vectors for Cancer Therapy. *Cancer Sci.* **2006**, *97*, 348–354.
5. Reischl, D.; Zimmer, A. Drug Delivery of siRNATherapeutics: Potentials and Limits of Nanosystems. *Nanomedicine (N. Y., NY, U. S.)* **2009**, *5*, 8–20.
6. Roy, I.; Stachowiak, M. K.; Bergey, E. J. Nonviral Gene Transfection Nanoparticles: Function and Applications in the Brain. *Nanomedicine (N. Y., NY, U. S.)* **2008**, *4*, 89–97.
7. Connor, E. E.; Mwamuka, J.; Gole, A.; Murphy, C. J.; Wyatt, M. D. Gold Nanoparticles Are Taken Up by Human Cells but Do Not Cause Acute Cytotoxicity. *Small* **2005**, *1*, 325–327.
8. Kuo, C.-W.; Lai, J.-J.; Wei, K. H.; Chen, P. Studies of Surface-Modified Gold Nanowires Inside Living Cells. *Adv. Funct. Mater.* **2007**, *17*, 3707–3714.
9. Shukla, R.; Bansal, V.; Chaudhary, M.; Basu, A.; Bhonde, R. R.; Sastry, M. Biocompatibility of Gold Nanoparticles and Their Endocytotic Fate Inside the Cellular Compartment: A Microscopic Overview. *Langmuir* **2005**, *21*, 10644–10654.
10. Pan, Y.; Neuss, S.; Leifert, A.; Fischler, M.; Wen, F.; Simon, U.; Schmid, G.; Brandau, W.; Jahnen-Dechent, W. Size-Dependent Cytotoxicity of Gold Nanoparticles. *Small* **2007**, *3*, 1941–1949.
11. Pan, Y.; Leifert, A.; Ruau, D.; Neuss, S.; Bornemann, J.; Schmid, G.; Brandau, W.; Simon, U.; Jahnen-Dechent, W. Gold Nanoparticles of Diameter 1.4 nm Trigger Necrosis by Oxidative Stress and Mitochondrial Damage. *Small* **2009**, *5*, 2067–2076.
12. Chithrani, B. D.; Chan, W. C. W. Elucidating the Mechanism of Cellular Uptake and Removal of Protein-Coated Gold Nanoparticles of Different Sizes and Shapes. *Nano Lett.* **2007**, *7*, 1542–1550.
13. Chithrani, B. D.; Ghazani, A. A.; Chan, W. C. W. Determining the Size and Shape Dependence of Gold Nanoparticle Uptake into Mammalian Cells. *Nano Lett.* **2006**, *6*, 662–668.
14. Yang, P.-H.; Sun, X.; Chiu, J.-F.; Sun, H.; He, Q.-Y. Transferrin-Mediated Gold Nanoparticle Cellular Uptake. *Bioconjugate Chem.* **2005**, *16*, 494–496.
15. Azzazy, H. M. E.; Mansour, M. M. H. In Vitro Diagnostic Prospects of Nanoparticles. *Clin. Chim. Acta* **2009**, *403*, 1–8.
16. Huang, X.; El-Sayed, I. H.; Qian, W.; El-Sayed, M. A. Cancer Cell Imaging and Photothermal Therapy in the Near-Infrared Region by Using Gold Nanorods. *J. Am. Chem. Soc.* **2006**, *128*, 2115–2120.
17. Brigger, I.; Dubernet, C.; Couvreur, P. Nanoparticles in Cancer Therapy and Diagnosis. *Adv. Drug Delivery Rev.* **2002**, *54*, 631–651.
18. Moghimi, S. M.; Szebeni, J. Stealth Liposomes and Long Circulating Nanoparticles: Critical Issues in Pharmacokinetics, Opsonization and Protein-Binding Properties. *Prog. Lipid Res.* **2003**, *42*, 463–478.
19. Boisselier, E.; Astruc, D. Gold Nanoparticles in Nanomedicine: Preparations, Imaging, Diagnostics, Therapies and Toxicity. *Chem. Soc. Rev.* **2009**, *38*, 1759–1782.
20. Kelly, K. L.; Coronado, E.; Zhao, L. L.; Schatz, G. C. The Optical Properties of Metal Nanoparticles: The Influence of Size, Shape, and Dielectric Environment. *J. Phys. Chem. B* **2002**, *107*, 668–677.
21. Hirsch, L. R.; Stafford, R. J.; Bankson, J. A.; Sershen, S. R.; Rivera, B.; Price, R. E.; Hazle, J. D.; Halas, N. J.; West, J. L. Nanoshell-Mediated Near-Infrared Thermal Therapy of Tumors under Magnetic Resonance Guidance. *Proc. Natl. Acad. Sci. U.S.A.* **2003**, *100*, 13549–13554.
22. Pitsillides, C. M.; Joe, E. K.; Wei, X.; Anderson, R. R.; Lin, C. P. Selective Cell Targeting with Light-Absorbing Microparticles and Nanoparticles. *Biophys. J.* **2003**, *84*, 4023–4032.
23. Bakhtiari Amir Bahman, S.; Hsiao, D.; Jin, G. Gates, Byron D.; Branda, Neil R. An Efficient Method Based on the Photothermal Effect for the Release of Molecules from Metal Nanoparticle Surfaces. *Angew. Chem., Int. Ed.* **2009**, *48*, 4166–4169.
24. Jain, P. K.; Qian, W.; El-Sayed, M. A. Ultrafast Cooling of Photoexcited Electrons in Gold Nanoparticle-Thiolated DNA Conjugates Involves the Dissociation of the Gold-Thiol Bond. *J. Am. Chem. Soc.* **2006**, *128*, 2426–2433.
25. Wijaya, A.; Schaffer, S. B.; Pallares, I. G.; Hamad-Schifferli, K. Selective Release of Multiple DNA Oligonucleotides from Gold Nanorods. *ACS Nano* **2008**, *3*, 80–86.
26. Barhoumi, A.; Huschka, R.; Bardhan, R.; Knight, M. W.; Halas, N. J. Light-Induced Release of DNA from Plasmon-Resonant Nanoparticles: Towards Light-Controlled Gene Therapy. *Chem. Phys. Lett.* **2009**, *482*, 171–179.
27. Jones, M. R.; Millstone, J. E.; Giljohann, D. A.; Seferos, D. S.; Young, K. L.; Mirkin, C. A. Plasmonically Controlled Nucleic Acid Dehybridization with Gold Nanoprisms. *ChemPhysChem* **2009**, *10*, 1461–1465.

28. Lee, S. E.; Liu, G. L.; Kim, F.; Lee, L. P. Remote Optical Switch for Localized and Selective Control of Gene Interference. *Nano Lett.* **2009**, *9*, 562–570.

29. Reismann, M.; Bretschneider, J. C.; Plessen, G. v.; Simon, U. Reversible Photothermal Melting of DNA in DNA-Gold-Nanoparticle Networks. *Small* **2008**, *4*, 607–610.

30. Stehr, J.; Hrelescu, C.; Sperling, R. A.; Raschke, G.; Wunderlich, M.; Nichtl, A.; Heindl, D.; Kurzinger, K.; Parak, W. J.; Klar, T. A.; Feldmann, J. Gold NanoStoves for Microsecond DNA Melting Analysis. *Nano Lett.* **2008**, *8*, 619–623.

31. Enüstün, B. V.; Turkevich, J. Coagulation of Colloidal Gold. *J. Am. Chem. Soc.* **1963**, *85*, 3317–3328.

32. Kimling, J.; Maier, M.; Okenve, B.; Kotaidis, V.; Ballot, H.; Plech, A. Turkevich Method for Gold Nanoparticle Synthesis Revisited. *J. Phys. Chem. B* **2006**, *110*, 15700–15707.

33. Liu, J.; Lu, Y. Preparation of Aptamer-Linked Gold Nanoparticle Purple Aggregates for colorimetric sensing of analytes. *Nat. Protoc.* **2006**, *1*, 246–252.

34. Hurst, S. J.; Lytton-Jean, A. K. R.; Mirkin, C. A. Maximizing DNA Loading on a Range of Gold Nanoparticle Sizes. *Anal. Chem.* **2006**, *78*, 8313–8318.

35. Kreibig, U.; Genzel, L. Optical Absorption of Small Metallic Particles. *Surf. Sci.* **1985**, *156* (Part 2), 678–700.

36. The values of T_m for the dsDNA complexes are reported by the supplier as 59 °C in aqueous 100 mM NaOAc, 63 °C in aqueous 200 mM NaOAc, and 67 °C in aqueous 200 mM NaOAc/50 mM MgSO4.